THE JOURNAL OF PHYSICAL CHEMISTRY C

ARTICLE

pubs.acs.org/JPCC

Enhanced Plasmonic Behavior of Incomplete Nanoshells: Effect of Local Field Irregularities on the Far-Field Optical Response

Ovidio Peña-Rodríguez*,†,‡ and Umapada Pal§

†Centro de Microanálisis de Materiales (CMAM), Universidad Autónoma de Madrid (UAM), Cantoblanco, E-28049 Madrid, Spain

‡Instituto de Óptica, Consejo Superior de Investigaciones Científicas (IO-CSIC), C/Serrano 121, E-28006 Madrid, Spain

§Instituto de Física, Benemérita Universidad Autónoma de Puebla, Apartado Postal J-48, Puebla, Puebla 72570, Mexico

ABSTRACT: Plasmonic behavior of core−shell-type nanostructures is currently the focus of intense research, particularly because of the tunable optical response of such materials suitable for emerging applications such as laser-induced interstitial thermotherapy, surface-enhanced Raman scattering, and biosensing. In this work, we report on the plasmonic behavior of incomplete nanoshells, providing insight into their evolution and growth. During the initial stages of formation, well-separated, noninteracting metallic nanoparticles at the surface of a dielectric core behave like isolated particles, but irregular and intense local electric fields (hot spots) are created when the number of metallic spheres increases, dramatically affecting the far-field optical response of the integral structure. Under the action of these local fields, the position of the surface plasmon resonance (SPR) suffers a dramatic red shift up to 50% higher than that of a complete nanoshell. The presented results open up the possibility of fabricating metallic nanoshells that are more efficient than the conventional ones for biological applications.

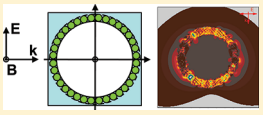

INTRODUCTION

Plasmonic behavior of metallic nanoparticles (NPs) is currently the subject of intense research because of the potential applications of such materials in many fields, including nonlinear optics, catalysis, chemical and biological sensing, and surface-enhanced Raman scattering (SERS).[1−6] Among plasmonic nanostructures, metallic nanoshells,[7] consisting of a dielectric core surrounded by a thin metal shell, have received wide attention because of their high stability; ease of preparation;[8] and superior performance in biological applications such as cancer treatment,[9,10] medical diagnostics,[11] and immunoassay.[12,13] Commonly, metal nanoshells are synthesized over silica particles of uniform sizes grown by the Stöber method.[14] Using successive chemical steps, the monodisperse silica cores are decorated with metal nanoparticles. The metal NPs are then allowed to grow until they intersect with each other, coalesce, and form a continuous metallic shell over the dielectric core.[8,15,16]

Although considerable effort has been devoted to fabricating such dielectric-core@metallic-shell nanostructures, it is still unclear how a complete nanoshell and its optical properties evolve from the primary metallic NPs to form a complete core−shell structure. This transition is often monitored through the linear optical response of the composite nanostructures, and the obtained optical responses are associated with the geometrical features of a continuous metallic nanoshell. However, it is very unlikely that a perfect and continuous shell layer can be formed through the coalescence of metal NPs, and some researchers argue that the obtained optical response in certain cases is produced not by a continuous layer but, rather, by clusters of metallic nanoparticles.[17−19] Arguments aside, there remains a reasonable question: Is it valid to use Mie theory to simulate the optical response of these nanostructures? It is striking that, despite these concerns, Mie theory is widely used to simulate the optical properties of metallic nanoshells, and the results are quite satisfactory.

In this work, we have simulated the optical response of metallic nanoshells at different stages of formation to elucidate how these systems evolve from the formation of discrete and isolated metal NPs over a dielectric core through the formation of a complete core−shell structure. In other words, we have investigated how the morphology of a metallic shell affects its optical properties. Bulk values of Au dielectric functions reported by Johnson and Christy[20] were used to calculate the optical responses, after application of the usual size correction.[21]

PROCEDURE

The studied system, depicted in Figure 1, consists of a silica core with a radius of 27.0 nm, over which spherical gold NPs of 5.0-nm radius were gradually added, until a complete shell formed. Initially, the particles were added with the criterion of maintaining maximum separation between them to avoid overlapping. With the selected radii of the silica and metal NPs, one can add up to 130 nonoverlapping Au spheres ($f \approx 0.52$), and in principle, all of the resulting configurations can be simulated by means of the T-matrix method.[22,23] However, we used this method to add only up to 100 spheres ($f \approx 0.4$), as recent experimental evidence[24] suggests that, for a ratio of center-to-center separation to effective diameter, $(R_A + R_B + d)/(R_A + R_B)$ (where R_A and R_B are the radii of two contiguous metallic NPs and d is the gap between them), below 1.05 the plasmon coupling does not continue to intensify with decreasing interparticle separation. From this point onward, the simulations were performed

Received: August 23, 2011
Revised: October 14, 2011
Published: October 18, 2011

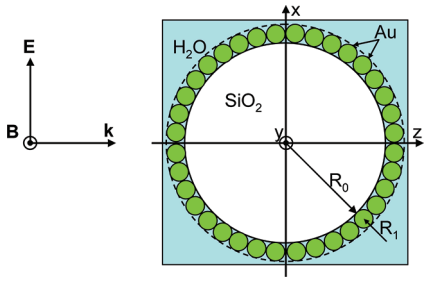

Figure 1. Schematic representation of the studied incomplete metallic nanoshells. **E** and **B** are the electric and magnetic fields, respectively, and **k** is the wavevector.

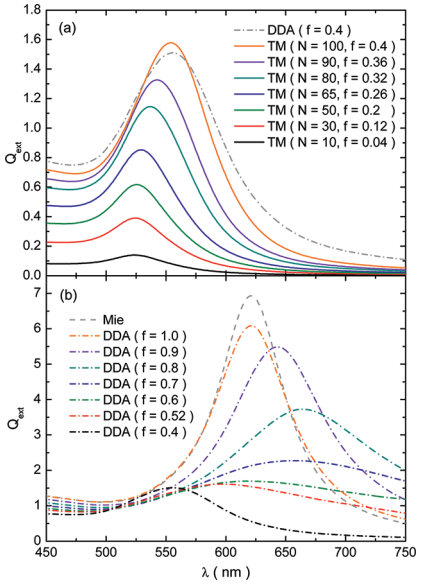

Figure 2. Simulated extinction efficiency for some selected intermediate configurations during the evolution of the system from isolated particles to the complete nanoshell, separated into (a) the initial low-variation region and (b) the regions where small changes of the filling factor produce dramatic spectral changes. The spectra were calculated using the T-matrix (solid lines), the discrete dipole approximation (dash-dotted lines), and Mie theory (dashed line).

using the code DDSCAT 7.0, which implements the discrete dipole approximation (DDA).[25] In the latter configurations, new particles were added randomly and allowed to overlap, until a continuous shell formed. The only exception was the geometry with $f \approx 0.52$, for which we used 130 nonoverlapping spheres for the DDA calculations. Finally, simulations of the complete nanoshell were performed using Mie theory,[26,27] for comparison purposes. The optimal dipole grid for DDA calculations was chosen by verifying that the calculated spectra for 100 nonoverlapping/intersecting spheres and a complete nanoshell were in good agreement with those obtained using the T-matrix (TM) and Mie theory, respectively. Good convergence was obtained for a dipole grid of 0.5 nm, confirming that the calculation of the efficiency factors has lower computational requirements than other problems.[28,29] Irrespective of the calculation method, all spectra were obtained by averaging over different orientations, to ensure that the considered system closely resembled the real systems. DDSCAT 7.0 was also used to calculate the electric field

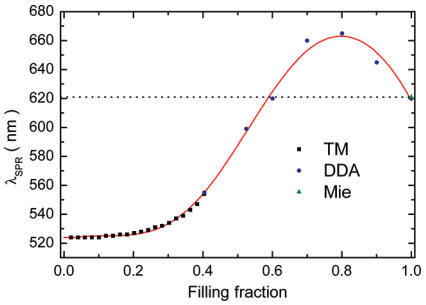

Figure 3. Calculated positions of the SPR peak as a function of the filling fraction, for incomplete metallic nanoshells. The horizontal dotted line represents the position of the SPR peak of the complete nanoshell. The red line is only a guide to the eyes.

near the vicinity of some incomplete gold nanoshells at localized surface plasmon resonance wavelengths.

Throughout this work, we use the term filling fraction, f (i.e., the ratio between the volume occupied by the incomplete nanoshell and that of the full nanoshell), to characterize the nanoshells. For the initial stages, when the Au spheres do not overlap, this quantity can be calculated as

$$f = \frac{NV_{sph}}{V_{sh}} = \frac{N{R_1}^3}{(R_0 + 2R_1)^3 - {R_0}^3} \quad (1)$$

where N is the number of gold spheres; V_{sph} and V_{sh} are the volumes of a single Au sphere and the complete nanoshell, respectively; and R_0 and R_1 are the radii of the silica and gold spheres, respectively. For the configurations with overlapping spheres, the filling fractions were simply calculated as

$$f = \frac{N_d^{is}}{N_d^{cs}} \quad (2)$$

where N_d^{is} and N_d^{cs} are the numbers of dipoles used to calculate the optical response of the incomplete and complete nanoshells, respectively.

RESULTS AND DISCUSSION

Figure 2 shows some selected optical extinction spectra, obtained during the evolution of the system from isolated particles over the silica core to a complete nanoshell. The variation of the peak position of the surface plasmon resonance (SPR) as a function of filling fraction is demonstrated in Figure 3. The spectra shown as solid lines in Figure 2a were calculated by means of the T-matrix; those presented as dash-dotted lines were obtained through the discrete dipole approximation (Figure 2a,b), and the spectrum shown in Figure 2b as a dashed line was calculated using Mie theory. The optical response in the first case (with a few gold spheres attached to the silica core) is virtually identical to that of isolated particles. Then, from around 65 gold spheres ($f \approx 0.26$) onward, a slight red shift of the SPR peak position occurs, showing that the gold particles begin to interact with their neighbors. This shift is relatively small until the metal particles start touching each other (and overlapping). Beyond that point, the SPR peak becomes wider and suffers larger red shifts. The trend continues until the filling fraction reaches 0.8, after which the trend reverses. The shifts observed for filling fractions above 0.6 are even greater than that obtained for a smooth and complete nanoshell. It should be noted that, in

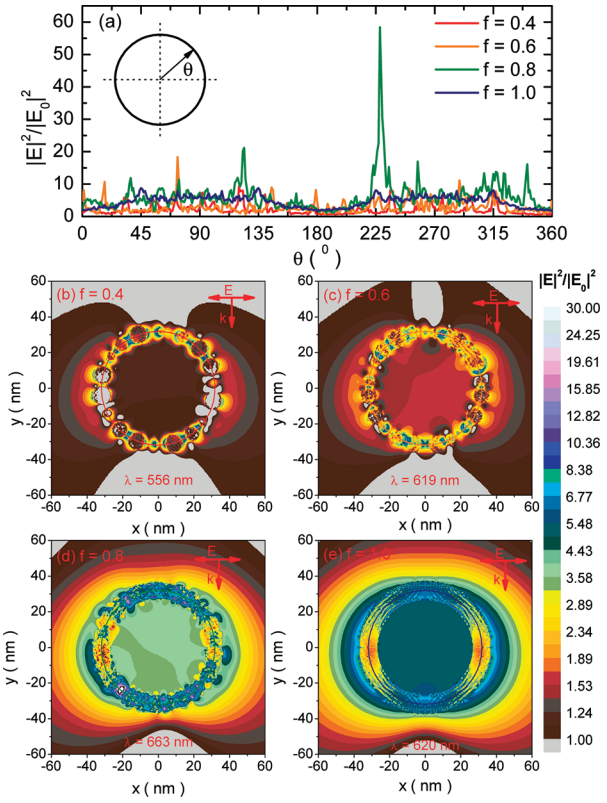

Figure 4. Near-field contour plots in the section plane for some incomplete gold nanoshells. The structures showed have filling fractions of (b) 0.4, (c) 0.6, (d) 0.8, and (e) 1.0. (a) The field profiles through the middle of the metallic shell (marked with solid lines in the contour plots) are also shown, for clarity.

principle, random ensembles of gold nanoparticles could produce spectra similar to those obtained in this work; however, we did not consider this possibility in our calculations because most current methods for the synthesis of nanoshells are mature enough to ensure that such agglomerates of particles are not produced.

As shown in Figure 4, the local electric field around a partially formed or incomplete shell is very irregular. In fact, for $f = 0.4$ (Figure 4b), the system basically behaves as a group of isolated particles. However, for filling fractions of 0.6 and 0.8 (particularly for the latter case), collective modes dominate the optical response. Interestingly, several "hot spots" can be seen over the incomplete nanoshells (more prominently for $f = 0.8$) that are very similar in nature to those observed in the gaps of metallic dimers.[30] We believe that these intense localized fields are responsible for the observed shifts in the SPR peak position. The phenomenon can be better understood by considering the SPR as a homogeneous electron gas oscillating over a fixed positive background, with the induced surface charges providing the restoring force. The presence of the hot spots produces a high charge density at those points. These high-charge-density points produce a greater electron screening and thus lead to a weaker restoring force of the electron gas, lowering its resonance frequency.

Both the SPR red shift and the appearance of hot spots around the metal NPs could have important implications for the application of metallic nanoshells. Whereas the red shift of the SPR peak is very important for the application of metal nanoshells in thermal treatment of tumors,[9,10] the appearance of

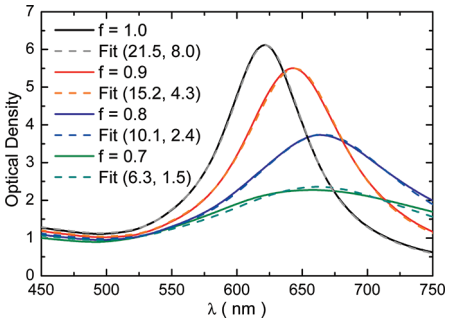

Figure 5. Optical extinction spectra of some incomplete gold nanoshells ($f = 0.7$, 0.8, 0.9, and 1.0), calculated using the DDA, and the corresponding fits, calculated using Mie theory.

hot spots in these nanostructures could prove interesting for surface-enhanced Raman scattering (SERS)[3,4] or some other applications that require intense local fields. However, a more detailed study, which is beyond the scope of the present work, is required to confirm or reject the feasibility of using rough metallic nanoshells in the aforementioned applications. On the other hand, it is very interesting that the "noisy" aspect of the near electric field is reflected in the far field only through the widening and shift of the SPR (i.e., the shape of the SPR remains approximately Lorentzian) (Figure 4a). This effect can be explained by the random nature of the irregularities in the local electric field, which are compensated when the contributions of various particles of different morphologies and orientations are averaged.

Finally, Figure 5 presents the optical extinction spectra of four incomplete gold nanoshells ($f = 0.7$, 0.8, 0.9, and 1.0), calculated using the DDA, and the corresponding fits obtained using Mie theory.[31] As can be seen, the obtained fits are excellent, particularly for the higher filling fractions ($f > 0.8$). However, the resulting geometrical parameters are completely wrong; that is, the thicknesses obtained for the silica core and the gold shells are not even close to those of the actual structure.[32] In other words, great care should be taken when interpreting the optical absorption spectra of nanoshells using Mie theory, as the obtained results could be completely misleading for incomplete metallic shells and shells with significant surface roughness. Therefore, it is important that experimentalists verify the quality of the obtained nanoshells through some alternative experimental technique before assuming that they are perfect multilayered spheres, as the consideration of light scattering alone is not enough to obtain the geometrical parameters in a reliable way.

In the literature, one can find previous works exposing some aspects analyzed in this work, such as the effect of surface roughness on the optical properties of nanoshells[33,34] or the evolution of their SPR during its formation.[35−37] For example, Wang et al.[33] used chemical etching to modify the surface of already formed nanoshells, finding a red shift of the SPR on increasing surface roughness similar to the one that we observed for filling fractions above 0.6. They interpreted the SPR shift as a reduction of the metal shell thickness. However, as explained earlier, our results indicate that the creation of local field irregularities also plays an important role in the observed red shifts. Lin and Sun,[34] on the other hand, performed a simulation similar to ours for Ag NPs and, somewhat surprisingly, concluded that "only the collective plasmon resonance mode in the continuous layer of metal shell is effective; the effect of surface morphology or roughness is minor".[34] The discrepancy

between their results and our calculations (which agree well with the experimental evidence[33]) probably has to do with the fact that they added the metal nanoparticles to the silica core in an ordered way, resulting in the formation of organized NP clusters, whereas we did it randomly. Moreover, some other groups[35−37] have reported the optical properties of semicontinuous gold and silver nanoshells, but none of them reported the evolution of the optical properties of the nanoshells for all possible filling fractions or established a close relationship between the hot spots and the red shift and widening of the SPR. Considering all of the factors involved, we believe that our results reflect a more realistic picture of the optical evolution of metallic nanoshells during the growth process.

CONCLUSIONS

We have presented the evolution of the optical response of metallic nanoshells during their formation and growth. It was found that the position of the SPR is barely affected until the metallic nanoparticles attached to the silica core begin to interact with each other ($f \approx 0.4$). For filling fractions higher than 0.6, the SPR position suffers dramatic red shifts, even exceeding the shift obtained for a perfect nanoshell. Whereas the obtained results serve as a warning on the indiscriminate use of Mie theory to interpret the results of optical absorption in multilayer plasmonic systems, they also open up the possibility of creating nanoshells tailored to the requirements of specific applications such as thermal ablation of tumors and surface-enhanced Raman scattering, to name only two.

AUTHOR INFORMATION

Corresponding Author

*E-mail: ovidio@bytesfall.com.

ACKNOWLEDGMENT

DDA calculations were carried out at the computer center of Instituto de Física, Universidad Autónoma de Puebla (IFUAP). O.P. R. thanks Consejo Nacional de Ciencia y Tecnología (CONACyT) of Mexico for extending a postdoctoral fellowship. This work was partially supported by Vicerrectoría de Investigación y Estudios de Posgrado-Benemérita Universidad Autónoma de Puebla (VIEP-BUAP) project grant 2011.

REFERENCES

(1) Oldenburg, S. J.; Westcott, S. L.; Averitt, R. D.; Halas, N. J. Surface enhanced Raman scattering in the near infrared using metal nanoshell substrates. *J. Chem. Phys.* **1999**, *111*, 4729.

(2) Jackson, J. B.; Westcott, S. L.; Hirsch, L. R.; West, J. L.; Halas, N. J. Controlling the surface enhanced Raman effect via the nanoshell geometry. *Appl. Phys. Lett.* **2003**, *82*, 257.

(3) Jackson, J. B.; Halas, N. J. Surface-enhanced Raman scattering on tunable plasmonic nanoparticle substrates. *Proc. Natl. Acad. Sci. U.S.A.* **2004**, *101*, 17930–17935.

(4) Lee, J.-H.; Mahmoud, M. A.; Sitterle, V. B.; Sitterle, J. J.; Meredith, J. C. Highly scattering, surface-enhanced Raman scattering-active, metal nanoparticle-coated polymers prepared via combined swelling−heteroaggregation. *Chem. Mater.* **2009**, *21*, 5654–5663.

(5) Alivisatos, P. The use of nanocrystals in biological detection. *Nat. Biotechnol.* **2004**, *22*, 47–52.

(6) Lal, S.; Westcott, S. L.; Taylor, R. N.; Jackson, J. B.; Nordlander, P.; Halas, N. J. Light interaction between gold nanoshells plasmon resonance and planar optical waveguides. *J. Phys. Chem. B* **2002**, *106*, 5609–5612.

(7) Averitt, R. D.; Sarkar, D.; Halas, N. J. Plasmon resonance shifts of Au-coated Au_2S nanoshells: Insight into multicomponent nanoparticle growth. *Phys. Rev. Lett.* **1997**, *78*, 4217.

(8) Oldenburg, S. J.; Averitt, R. D.; Westcott, S. L.; Halas, N. J. Nanoengineering of optical resonances. *Chem. Phys. Lett.* **1998**, *288*, 243–247.

(9) Hirsch, L. R.; Stafford, R. J.; Bankson, J. A.; Sershen, S. R.; Rivera, B.; Price, R. E.; Hazle, J. D.; Halas, N. J.; West, J. L. Nanoshell-mediated near-infrared thermal therapy of tumors under magnetic resonance guidance. *Proc. Natl. Acad. Sci. U.S.A.* **2003**, *100*, 13549–13554.

(10) Zhang, J. Z. Biomedical applications of shape-controlled plasmonic nanostructures: A case study of hollow gold nanospheres for photothermal ablation therapy of cancer. *J. Phys. Chem. Lett.* **2010**, *1* 686–695.

(11) Allain, L. R.; Vo-Dinh, T. Surface-enhanced Raman scattering detection of the breast cancer susceptibility gene BRCA1 using a silver-coated microarray platform. *Anal. Chim. Acta* **2002**, *469*149–154.

(12) Hirsch, L. R.; Jackson, J. B.; Lee, A.; Halas, N. J.; West, J. L. A whole blood immunoassay using gold nanoshells. *Anal. Chem.* **2003**, *75* 2377–2381.

(13) Cui, Y.; Ren, B.; Yao, J.-L.; Gu, R.-A.; Tian, Z.-Q. Synthesis of $Ag_{core}−Au_{shell}$ bimetallic nanoparticles for immunoassay based on surface-enhanced Raman spectroscopy. *J. Phys. Chem. B* **2006**, *110* 4002–4006.

(14) Stöber, W.; Fink, A.; Bohn, E. Controlled growth of monodisperse silica spheres in the micron size range. *J. Colloid Interface Sci.* **1968**, *26*, 62–69.

(15) Westcott, S. L.; Oldenburg, S. J.; Lee, T. R.; Halas, N. J. Formation and adsorption of clusters of gold nanoparticles onto functionalized silica nanoparticle surfaces. *Langmuir* **1998**, *14*, 5396–5401.

(16) Graf, C.; van Blaaderen, A. Metallodielectric colloidal core−shell particles for photonic applications. *Langmuir* **2002**, *18*, 524–534.

(17) Raschke, G.; Brogl, S.; Susha, A. S.; Rogach, A. L.; Klar, T. A.; Feldmann, J.; Fieres, B.; Petkov, N.; Bein, T.; Nichtl, A.; Kurzinger, K. Gold nanoshells improve single nanoparticle molecular sensors. *Nano Lett.* **2004**, *4*, 1853–1857.

(18) Zhang, J. Z.; Schwartzberg, A. M.; Norman; Grant, C. D.; Liu, J.; Bridges, F.; van Buuren, T. Comment on "Gold nanoshells improve single nanoparticle molecular sensors". *Nano Lett.* **2005**, *5*, 809–810.

(19) Raschke, G.; Brogl, S.; Susha, A. S.; Rogach, A. L.; Klar, T. A.; Feldmann, J.; Fieres, B.; Petkov, N.; Bein, T.; Nichtl, A.; Kürzinger, K. Reply to "Comment on 'Gold nanoshells improve single nanoparticle molecular sensors'". *Nano Lett.* **2005**, *5*, 811–812.

(20) Johnson, P. B.; Christy, R. W. Optical constants of the noble metals. *Phys. Rev. B* **1972**, *6*, 4370–4379.

(21) Peña, O.; Pal, U.; Rodríguez-Fernández, L.; Crespo-Sosa, A. Linear optical response of metallic nanoshells in different dielectric media. *J. Opt. Soc. Am. B* **2008**, *25*, 1371–1379.

(22) Mackowski, D. W. Calculation of total cross sections of multiple-sphere clusters. *J. Opt. Soc. Am. A* **1994**, *11*, 2851–2861.

(23) Mackowski, D. W.; Mishchenko, M. I. Calculation of the T matrix and the scattering matrix for ensembles of spheres. *J. Opt. Soc. Am. A* **1996**, *13*, 2266–2278.

(24) Yang, L.; Wang, H.; Yan, B.; Reinhard, B. M. Calibration of silver plasmon rulers in the 1−25 nm separation range: Experimental indications of distinct plasmon coupling regimes. *J. Phys. Chem. C* **2010**, *114*, 4901–4908.

(25) Draine, B. T. The discrete-dipole approximation and its application to interstellar graphite grains. *Astrophys. J.* **1988**, *333*, 848.

(26) Yang, W. Improved recursive algorithm for light scattering by a multilayered sphere. *Appl. Opt.* **2003**, *42*, 1710–1720.

(27) Peña, O.; Pal, U. Scattering of electromagnetic radiation by a multilayered sphere. *Comput. Phys. Commun.* **2009**, *180*, 2348–2354.

(28) Draine, B. T.; Flatau, P. J. Discrete-dipole approximation for scattering calculations. *J. Opt. Soc. Am. A* **1994**, *11*, 1491–1499.

(29) Xing, Z.; Hanner, M. S. Light scattering by aggregate particles. *Astron. Astrophys.* **1997**, *324*, 805–820.

(30) Xu, H.; Käll, M. Surface-plasmon-enhanced optical forces in silver nanoaggregates. *Phys. Rev. Lett.* **2002**, *89*, 246802.

(31) Peña-Rodríguez, O.; González Pérez, P. P.; Pal, U. MieLab: A software tool to perform calculations on the scattering of electromagnetic waves by multilayered spheres. *Int. J. Spectrosc.* **2011**, *2011*, 583743.

(32) A small part of the discrepancy stems from the calculation error in the DDA method, as can be seen in the case of a complete nanoshell; however, the geometrical parameters obtained for the other cases are so different that this error alone cannot explain them.

(33) Wang, H.; Goodrich, G. P.; Tam, F.; Oubre, C.; Nordlander, P.; Halas, N. J. Controlled texturing modifies the surface topography and plasmonic properties of Au nanoshells. *J. Phys. Chem. B* **2005**, *109* 11083–11087.

(34) Lin, Q.; Sun, Z. Optical extinction properties of aggregated ultrafine silver nanoparticles on silica nanospheres. *J. Phys. Chem. C* **2011**, *115*, 1474–1479.

(35) Peceros, K. E.; Xu, X.; Bulcock, S. R.; Cortie, M. B. Dipole–dipole plasmon interactions in gold-on-polystyrene composites. *J. Phys. Chem. B* **2005**, *109*, 21516–21520.

(36) Rohde, C. A.; Hasegawa, K.; Deutsch, M. Coherent light scattering from semicontinuous silver nanoshells near the percolation threshold. *Phys. Rev. Lett.* **2006**, *96*, 045503.

(37) Preston, T. C.; Signorell, R. Growth and optical properties of gold nanoshells prior to the formation of a continuous metallic layer. *ACS Nano* **2009**, *3*, 3696–3706.